

Exploring the mechanism of action of herb pair *Pinellia Ternata-Magnolia Officinalis* in the treatment of liver cancer based on network pharmacology and molecular docking

Zi-Wei Du^{1,2#}, Meng-Wei Xu^{1,2#}, Rui Peng^{1,2#}, Min Fang^{1,2}, Yan Liu^{1,2}, Guang-Shuai Zhang^{1,2}, Si Yan^{1,2}, Li-Na Yang^{3*}, Shuang-Lin Qin^{1,2*}

¹School of Pharmacy, Xianning Medical College, Hubei University of Science and Technology, Xianning 437100, China. ²Hubei Engineering Research Center of Traditional Chinese Medicine of South Hubei Province, Xianning Medical College, Hubei University of Science and Technology, Xianning 437100, China.

³Department of Pharmacy, Zhangzhou Affiliated Hospital of Fujian Medical University, Zhangzhou 363000, China.

#These authors contributed equally to this work and are co-first authors for this paper.

*Correspondence to: Shuanglin Qin, Hubei Engineering Research Center of Traditional Chinese Medicine of South Hubei Province, Xianning Medical College, Hubei University of Science and Technology, No.88, Xianning Avenue, Xianning 437100, China. E-mail: shuanglin@tju.edu.cn; Li-Na Yang, Department of Pharmacy, Zhangzhou Affiliated Hospital of Fujian Medical University, No.59, Shengli Road, Zhangzhou 363000, China. E-mail: ylnzys@163.com.

Author contributions

Qin SL and Yang LN share responsibility for the entire manuscript; Du ZW, Xu MW, Peng R and Fang M, Liu Y, Zhang GS and Yan S designed, wrote, and revised the manuscript; Du ZW and Fang M contributed to drawing the diagram; Qin SL, Yang LN, Du ZW and Fang M reviewed the manuscript and provided financial support. All authors read and approved the final version of the submitted manuscript.

Competing interests

The authors declare no conflicts of interest.

Acknowledgments

This research was funded by the National Natural Science Foundation of China (No. 82204250); China Postdoctoral Science Foundation (No. 2021M693961); Young and Middle-Aged Talent Project of Hubei Provincial Department of Education (No. Q20222808); Hubei University of Science and Technology Doctoral Startup Fund Project (No. BK202029); Outstanding Young and Middle-Aged Scientific and Technological Innovation Team in Colleges and Universities in Hubei Province (No. T2021022).

Peer review information

Pharmacology Discovery thanks all anonymous reviewers for their contribution to the peer review of this paper.

Abbreviations

BX-HP, Herb pair *Pinellia ternate-Magnolia officinalis*; BC, Binding energy; MD, Molecular dynamic simulation.

Citation

Du ZW, Xu MW, Peng R, et al. Exploring the mechanism of action of herb pair *Pinellia Ternata-Magnolia Officinalis* in the treatment of liver cancer based on network pharmacology and molecular docking. *Pharmacol Discov.* 2024;4(1):6. doi: 10.53388/PD202404006.

Executive editor: Ting Yu.

Received: 31 January 2024; Accepted: 07 March 2024;

Available online: 13 March 2024.

© 2024 By Author(s). Published by TMR Publishing Group Limited. This is an open access article under the CC-BY license. (<https://creativecommons.org/licenses/by/4.0/>)

Abstract

Background: Explore the anti-tumor mechanism of herb pair *Pinellia ternate-Magnolia officinalis* (BX-HP) in liver cancer through network pharmacology using molecular docking methods. **Method:** The active ingredients and corresponding targets of the herb pair *Pinellia ternate-Magnolia officinalis* were obtained from the HERB database. The relevant targets for liver cancer were obtained from GeneCards, DisGeNET, TTD, and Drugbank databases. Obtain common targets between herb pair *Pinellia ternate-Magnolia officinalis* and liver cancer through the Bioinformatics platform, establish a PPI network diagram using STRING software, and perform GO functional enrichment and KEGG pathway enrichment analysis on the DAVID platform. AutoDockTools 1.5.7 software and molecular dynamics simulation analysis are used to evaluate the binding of components to target proteins. HERB database, SwissTargetPrediction database, SwissADME database, UniProt database, GeneCards database, TTD database, DRUGBANK database, DisGeNET database, String, DAVID. Bioinformatics platform, PDB database, PubChem and TCMSp database. **Result:** A total of 22 active ingredients with a Probability > 0.1 targets in *Magnolia officinalis* were screened, 26 active ingredients with a Probability > 0.1 targets in *Pinellia ternata*, ten vital active ingredients, corresponding to 979 and 803 targets with a Probability > 0.1 targets, 2536 liver cancer-related targets, and 279 targets in the herb pair *Pinellia ternate-Magnolia officinalis*. The GO functional enrichment analysis resulted in 1297 entries, namely 971 biological process entries, 118 cell localization entries, and 208 molecular function entries. Three signaling pathways were annotated through the KEGG pathway. Based on molecular docking, ten vital active ingredients and five target proteins were validated to exhibit an excellent binding affinity. The above data indicates that combining the herb pair *Pinellia ternate-Magnolia officinalis* may treat liver cancer through specific targets and signaling pathways. **Conclusion:** Herb pair *Pinellia ternate-Magnolia officinalis* has a synergistic effect on treating liver cancer through multicomponent, multitarget, and multi-pathway approaches. This study provides a sufficient theoretical basis for subsequent research.

Keywords: liver cancer; herb pair *Pinellia ternate-Magnolia officinalis*; target prediction; network pharmacology; molecular docking; mechanism

Introduction

Hepatocellular carcinoma (HCC) is a common malignant tumor in the digestive system, which has become the fourth most common malignant tumor and the second leading cause of tumor mortality in China [1]. In clinical practice, it is often based on the symptoms exhibited by patients with liver cancer, belonging to the categories of traditional Chinese medicine such as "liver accumulation jaundice," "accumulation syndrome," as well as "flank pain and bloating," etc. [2]. Characterized by a mixture of deficiency and excess, it first appeared in the *Yellow Emperor's Inner Canon*, with deficiencies being more than reality. Traditional Chinese medicine treatment usually focuses on strengthening the foundation and eliminating pathogenic factors [3]. Modern doctors have different views on its etiology and pathogenesis from the perspective of spleen deficiency, qi stagnation, blood stasis, and cancer toxin. The invasion and metastasis of liver cancer are fundamental reasons for the failure of its clinical treatment. Therefore, how to effectively inhibit the invasion and metastasis of liver cancer has become a research hotspot in recent years [2]. Traditional Chinese medicine has advantages in treating liver cancer, such as anti-tumor effects, enhanced immunity, and improved clinical symptoms [4]. Traditional Chinese medicine has played an essential and unique role in the prevention and treatment of liver cancer in China. With the deepening and changing concept of modern medicine in tumor treatment, the role and mechanism of traditional Chinese medicine in preventing and treating liver cancer recurrence as well as metastasis have been increasingly valued by clinical and academic circles.

The name *Pinellia ternata* came from the "Rituals-Monthly Order": "In May *Pinellia ternata* is born" [5]. *Pinellia ternata*, dry and phlegmatic, is a crucial medicine for treating dampness and phlegm, as well as eliminating swelling and dispersing knots; it is widely used in the compound formulas of *Treatise on Cold-Attack, Synopsis of Golden Chamber*, and other medical books. Modern research shows that *Pinellia ternata* contains alkaloids, organic acids, flavonoids, and many other chemical components, of which alkaloids are the main active ingredients of *Pinellia ternata*, with anti-tumor, antiemetic, anticonvulsant, sedative and hypnotic effect, etc [6]. Experiments on animal and cellular models have shown that the active ingredients of *Pinellia ternata* have a significant inhibitory effect on hepatocellular carcinoma, whose anti-tumor mechanisms are also diverse. *Magnolia officinalis* is a plant of the Magnoliaceae family, which has been proven to have an excellent inhibitory effect on liver cancer tumor cells. Among them, the anti-tumor effect of magnolol, the main active ingredient, has been confirmed in many studies. The active ingredients of *Pinellia ternata* and *Magnolia officinalis* have inhibitory effects on a variety of malignant tumor cells, which fully indicates that they exert their anti-tumor efficacy in a multi-component, multi-target, and multi-pathway form, laying a foundation for its herb pair *Pinellia ternate-Magnolia officinalis* medicinal anti-tumor research [7].

Network pharmacology can be used to predict the action mechanism of drugs in the treatment of diseases from a holistic perspective, similar to the multi-component and multi-target action mechanism of traditional Chinese medicine (TCM) compounding, which is in line with the principle of the holistic concept of TCM [8]. Molecular docking can elucidate the action mechanism between ligands and receptors at the molecular level and further analyze and identify the consequences of network pharmacology. Cyber-pharmacological studies are based on mathematical and complex network models, which can abstractly express the interactions of herbal formulas in various organism systems in the form of networks. Cyber-pharmacological studies based on the combination of techniques such as cyber-pharmacology and molecular docking accurately predict the action mechanism of drugs in treating diseases. At the same time, different active ingredients act through different pathways by regulating other target proteins to achieve therapeutic goals, reflecting the multi-component, multi-target, and

multi-pathway characteristics of Chinese medicine [9]. This paper used the network pharmacology and molecular docking method to analyze the molecular mechanism of the anti-tumor effect of herb pair *Pinellia ternate-Magnolia officinalis* on liver cancer, which provides a sufficient theoretical basis for subsequent studies. The working flowchart is shown in Figure 1.

Materials and methods

Databases and software

Databases. HERB Herbal Compendium (<http://herb.ac.cn/>) [10]. SwissTargetPrediction database (<http://www.swisstargetprediction.ch/>) [11]. SwissADME database (<http://www.swissadme.ch/>) [12]. UniProt database (<https://www.uniprot.org/>) [13]. GeneCards database (<https://www.genecards.org/>) [14]. TTD database (<https://db.idrblab.net/ttd/>) [15]. DRUGBANK database (<https://go.drugbank.com/>) [16]. DisGeNET database (<https://www.disgenet.org/>) [17]. String (<https://cn.string-db.org/>) [18]. DAVID (<https://david.ncicrf.gov/summary.jsp>) [19]. The bioinformatics platform (<https://www.bioinformatics.com.cn/>) [20]. PDB database (<https://www.rcsb.org/>) [21]. PubChem (<https://pubchem.ncbi.nlm.nih.gov/>) and TCMSP database (<https://tcmispw.com/tcmisp.php>) [22, 23].

Software. Cytoscape 3.10.1 software (<https://cytoscape.org/>) [24]. AutoDockTools 1.5.7 software (<https://autodock.scripps.edu/>) [25]. OpenBabel 13.1 software (https://openbabel.org/wiki/Main_Page), PyMOL software (<https://pymol.org/2/>) and Chemdraw [26, 27].

Component and target screening of *Pinellia ternata-Magnolia officinalis*

The search of the HERB database was utilized to retrieve the active constituents of *Pinellia ternata-Magnolia officinalis*, respectively. Meanwhile, the screening was continued to obtain the active constituents of herb pair *Pinellia ternate-Magnolia officinalis* based on the Lipinski five principles ($M_w \leq 500$, $miLogP \leq 5$, $nOHNH \leq 5$, $nOH \leq 10$) with $M_w \leq 500$. The obtained active ingredients were imported into the PubChem database to continue screening the principal components according to Lipinski's five principles for further screening in the SwissADME database, following the GI absorption of High, Lipinski, Ghosc, Vrber, Ean, and Megge, adding up to at least three YES. The principal components of SMILES were input into the SwissTargetPrediction database to screen targets with a possibility > 0.1.

Screening of liver-cancer-related targets

Search the databases GeneCards, DisGeNET, TTD, and Drugbank using the keyword "liver cancer" to obtain liver-cancer-related targets. Convert the duplicated liver cancer targets into corresponding genes using the Uniprot database and correct them to official names. Intersect the liver cancer targets obtained from the above four databases using a microbiome platform and intersect the drug ingredient targets with liver-cancer-related disease targets to obtain common targets for both.

Building protein-protein interaction networks

Import the common targets of *Pinellia ternate-Magnolia officinalis* and liver cancer into the String database. Select the species as homo sapiens, set the confidence level of target association as 0.9, and construct a protein-protein interaction (PPI) network for the target network. Download the TVS-format file of PPIs from the String database, import the file into Cytoscape 3.10.1 software for visualization, and use the CentiScaPe2.2 plugin to filter critical targets based on Degree, Betweenness, and Closeness values to obtain the diagrams of the PPI network and primary target information.

GO and KEGG analysis

Use the DAVID platform to input common targets for drugs and diseases. Click on "Official Gene Symbol" and "GeneList" in sequence,

and select the species "Homo sapiens". Mainly analyze the biological process (BP), cell composition (CC), molecular function (MF), and signaling pathways of the targets, and utilize the microbiome platform (<https://www.bioinformatics.com.cn/>) to visualize the results.

Molecular docking

Molecular docking was performed on the core anti-tumor targets and corresponding active components of the herb pair *Pinellia ternate-Magnolia officinalis* in liver cancer. Download the functional ingredient structures from the PubChem database (<https://pubchem.ncbi.nlm.nih.gov/>). Download the SDF structure of active ingredients from the TCMSP database (<https://tcmspw.com/tcmsp.php>). Download the active ingredients of core proteins in the mol2 format from the PDB database (<https://www.rcsb.org/>). The PDB IDs were as follows: 6NJS (STAT3), 3O96 (AKT1), 1BYQ (HSP90AA1), 4U5J (SRC), and 8EXL (PIK3CA).

Use OpenBabel software to convert the SDF structure of the active ingredients into "mol2" for use. Use PyMOL software (<https://www.Pymol.org>) and AutoDock Tools-1.5.7 software (<https://autodock.scripps.edu/resources>), to dehydrate and hydrogenate proteins. Convert the formats of active ingredients and target proteins to the PDBQT format. Use AutoDock Tools-1.5.7 software to combine the processed proteins with their corresponding active ingredients to obtain binding energy. A binding energy of < 0 indicates that the ligands and receptors can spontaneously bind and that the conformation with the lowest binding energy is optimal. By combining the docking values, active ingredients and targets with better integration activity can be screened. The higher the binding energy is an absolute value, the stronger the docking ability is, and the higher the molecular stability will be after docking [28]. Finally, the molecular docking results are visualized using LigPlus software.

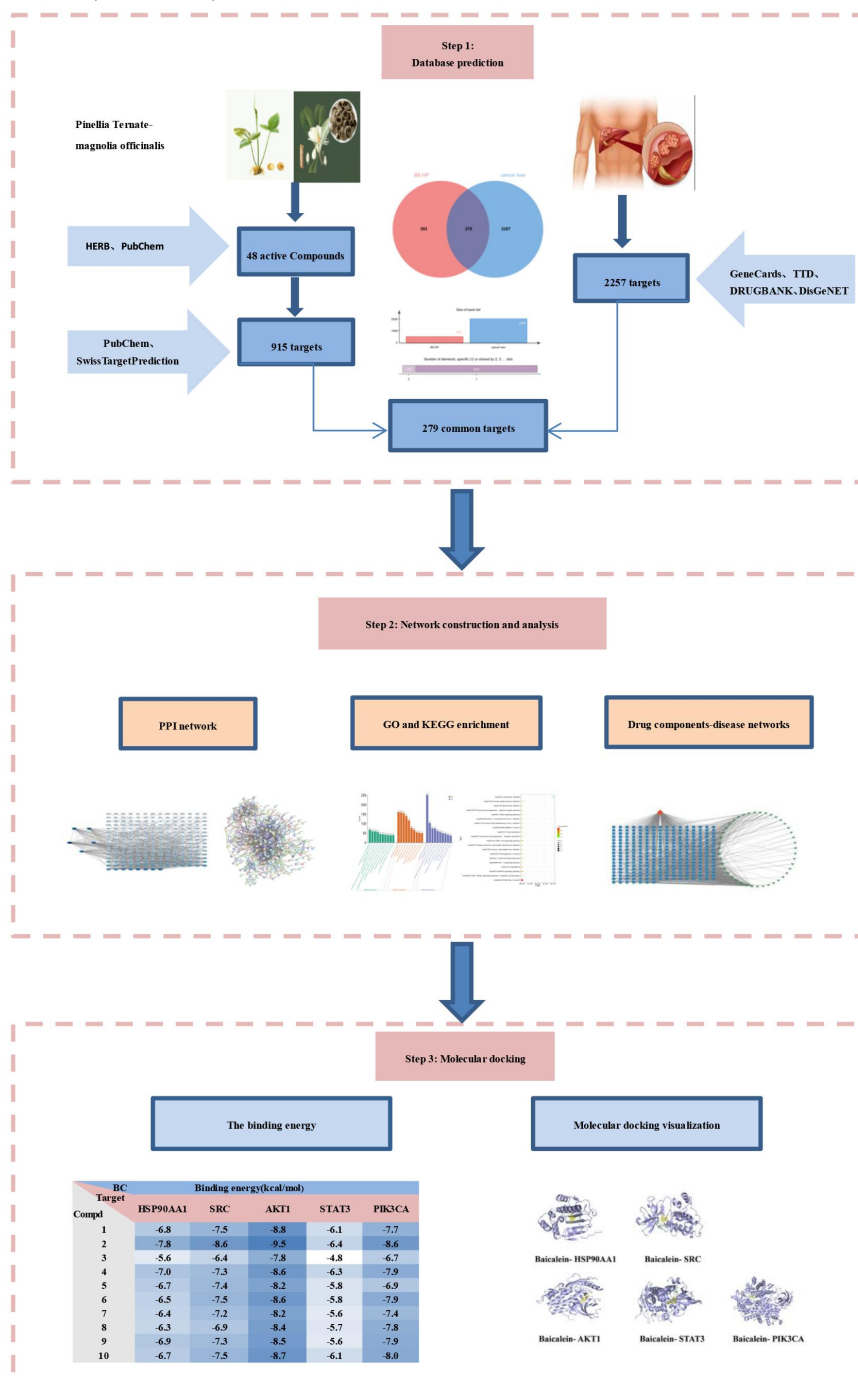


Figure 1 Flow diagram of the research

Results

Active ingredients and predicted targets of herb pair *Pinellia ternata*-*Magnolia officinalis*

The HERB database retrieved 179 components of *Pinellia ternata* and 93 components of *Magnolia officinalis*. According to the Lipinski Five Principles ($M_w \leq 500$, $\text{miLogP} \leq 5$, $\text{nOHNH} \leq 5$, $\text{nOH} \leq 10$), $M_w \leq 500$ was further screened to obtain the main components of *Pinellia ternata* and *Magnolia officinalis*, resulting in 43 principal components of *Magnolia officinalis* and 98 main components of *Pinellia ternata*. Import the PubChem CID of the main components into the PubChem database and screen according to the Lipinski five principles, resulting

in 40 active ingredients of *Magnolia officinalis* and 51 active ingredients of *Pinellia ternata*. Then, these components were screened in the SwissADME database, following the GI absorption of High, Lipinski, Ghost, Vrber, Ean, and Megge, with at least three YES, resulting in 33 active ingredients of *Magnolia officinalis* and 44 active ingredients of *Pinellia ternata*. Further, the SMILES of the principal components obtained from the above screening into the SwissTargetPrediction database for further screening for components with a Probability > 0.1 targets, 22 active ingredients of *Magnolia officinalis* and 26 active ingredients of *Pinellia ternata* were obtained (Table 1). The target with a Probability > 0.1 was deduplicated, resulting in 426 and 489 targets corresponding to Houpu and Banxia, respectively.

Table 1 Active constituents of targets with Probability > 0.1

NO.	Molecules name	Formula	PubChem CID
BX1	Catechol	C ₆ H ₆ O ₂	289
BX2	Guanine	C ₅ H ₅ N ₅ O	135398634
BX3	Chrysophanic acid	C ₁₅ H ₁₀ O ₄	10208
BX4	Vanillic Acid	C ₈ H ₈ O ₄	8468
BX5	Glutamic Acid	C ₅ H ₉ NO ₄	33032
BX6	protocatechuic acid	C ₇ H ₆ O ₄	72
BX7	1,5-Pentanediol	C ₅ H ₁₂ O ₂	8105
BX8	Baicalein	C ₁₅ H ₁₀ O ₅	5281605
BX9	Scopoletin	C ₁₀ H ₈ O ₄	5280460
BX10	D-Methionine	C ₅ H ₁₁ NO ₂ S	84815
BX11	9H-Pyrido[3,4-B]indole	C ₁₁ H ₈ N ₂	64961
BX12	p-Anisic acid	C ₈ H ₈ O ₃	7478
BX13	6-shogaol	C ₁₇ H ₂₄ O ₃	5281794
BX14	Anethole	C ₁₀ H ₁₂ O	637563
BX15	D-2-Aminobutyric acid	C ₄ H ₉ NO ₂	439691
BX16	(-)-Coniine	C ₈ H ₁₇ N	638021
BX17	DL-Tyrosine	C ₉ H ₁₁ NO ₃	1153
BX18	2-(Hydroxymethyl)-6-[4-(3-hydroxyprop-1-enyl)-2-methoxyphenoxy]oxane-3,4,5-triol	C ₁₆ H ₂₂ O ₈	3496897
BX19	cis-p-Coumaric acid	C ₉ H ₈ O ₃	1549106
BX20	3,4-Dihydroxybenzoate	C ₇ H ₅ O ₄	54675866
BX21	9-Oxononanoic acid	C ₉ H ₁₆ O ₃	75704
BX22	Cavidine	C ₂₁ H ₂₃ NO ₄	193148
BX23	(R)-3-Aminobutanoic Acid	C ₄ H ₉ NO ₂	5706670
BX24	isolariciresino	C ₂₀ H ₂₄ O ₆	11631864
BX25	cyclo-(leu-tyr)	C ₁₅ H ₂₀ N ₂ O ₃	15550385
BX26	conimine	C ₂₂ H ₃₆ N ₂	551152
HP1	magnolol	C ₁₈ H ₁₈ O ₂	72300
HP2	sinapic acid	C ₁₁ H ₁₂ O ₅	637775
HP3	β-eudesmol	C ₁₅ H ₂₆ O	91457
HP4	(+)-α-Terpineol	C ₁₀ H ₁₈ O	442501
HP5	honokiol	C ₁₈ H ₁₈ O ₂	72303
HP6	α-santalol	C ₁₅ H ₂₄ O	24832102
HP7	α-Eudesmol	C ₁₅ H ₂₆ O	92138
HP8	Elemol	C ₁₅ H ₂₆ O	92762
HP9	anonaine	C ₁₇ H ₁₅ NO ₂	160597
HP10	magnolignan c	C ₁₈ H ₂₀ O ₄	5319203
HP11	β-humulene	C ₁₅ H ₂₄	21159064
HP12	magnaldehyde e	C ₁₆ H ₁₄ O ₃	5319190
HP13	magnaldehyde d	C ₁₆ H ₁₄ O ₃	5319189
HP14	Magnograndiolide	C ₁₅ H ₂₂ O ₄	5319198
HP15	magnolignan a	C ₁₈ H ₂₀ O ₄	5319201
HP16	Michelenolide	C ₁₅ H ₂₀ O ₄	442278
HP17	randainal	C ₁₈ H ₁₆ O ₃	5320888
HP18	Asimilobine	C ₁₇ H ₁₇ NO ₂	25774982
HP19	[3R, (+)]-1,2,3,4,5,6,7,8-Octahydro-α,α,3β,8β-tetramethyl-5β-azulenemethanol	C ₁₅ H ₂₆ O	72607
HP20	(2S,3R)-2-(hydroxymethyl)-5-(2-hydroxy-5-prop-2-enylphenyl)-2,3-dihydro-1-benzofuran-3-ol	C ₁₈ H ₁₈ O ₄	15714551
HP21	magnolignan b	C ₁₈ H ₂₀ O ₅	5319202
HP22	(E)-3-[3-[5-(2,3-dihydroxypropyl)-2-hydroxyphenyl]-4-hydroxyphenyl]prop-2-enal	C ₁₈ H ₁₈ O ₅	5319188

Screening results of liver cancer gene targets

The GeneCards database obtained 1,350 liver cancer-related targets with a correlation score of ≥ 19 . TTD, DRUGBANK, and DisGeNET databases were supplemented with a correlation score of ≥ 0.04 to obtain 61, 2, and 1912 related targets, respectively. Merge and remove duplicates from the 4 data targets to obtain 2257 liver-cancer-related targets, which were then standardized as gene symbols through UniProt proofreading.

Integrating herb pair *Pinellia ternata-Magnolia officinalis* with liver-cancer-related targets resulted in 279 common targets, which served as potential targets for treating liver cancer with herb pair *Pinellia ternata-Magnolia officinalis*. A Venn diagram was drawn through an online network (Figure 2).

Construction and analysis of liver cancer PPI network

Draw a PPI network diagram of drug-disease intersection targets by inputting common targets into the STRING platform (Figure 3). Save the obtained results in the tsv format and import them into Cytoscape 3.10.1 software. Use the CentiScaPe2.2 plugin to filter those targets based on the "Degree," "Betweenness," and "Closeness" conditions. Visualize the targets according to the calculated Degree value. The nodes increased in size as the degree value increased, with the color changing from dark blue to light blue. The top 4 genes regarding degree ranking were HSP90AA1, SRC, AKT1, STAT3, and PIK3CA, which were the core targets of the herb pair *Pinellia ternata-Magnolia officinalis* with therapeutic effects on liver cancer.

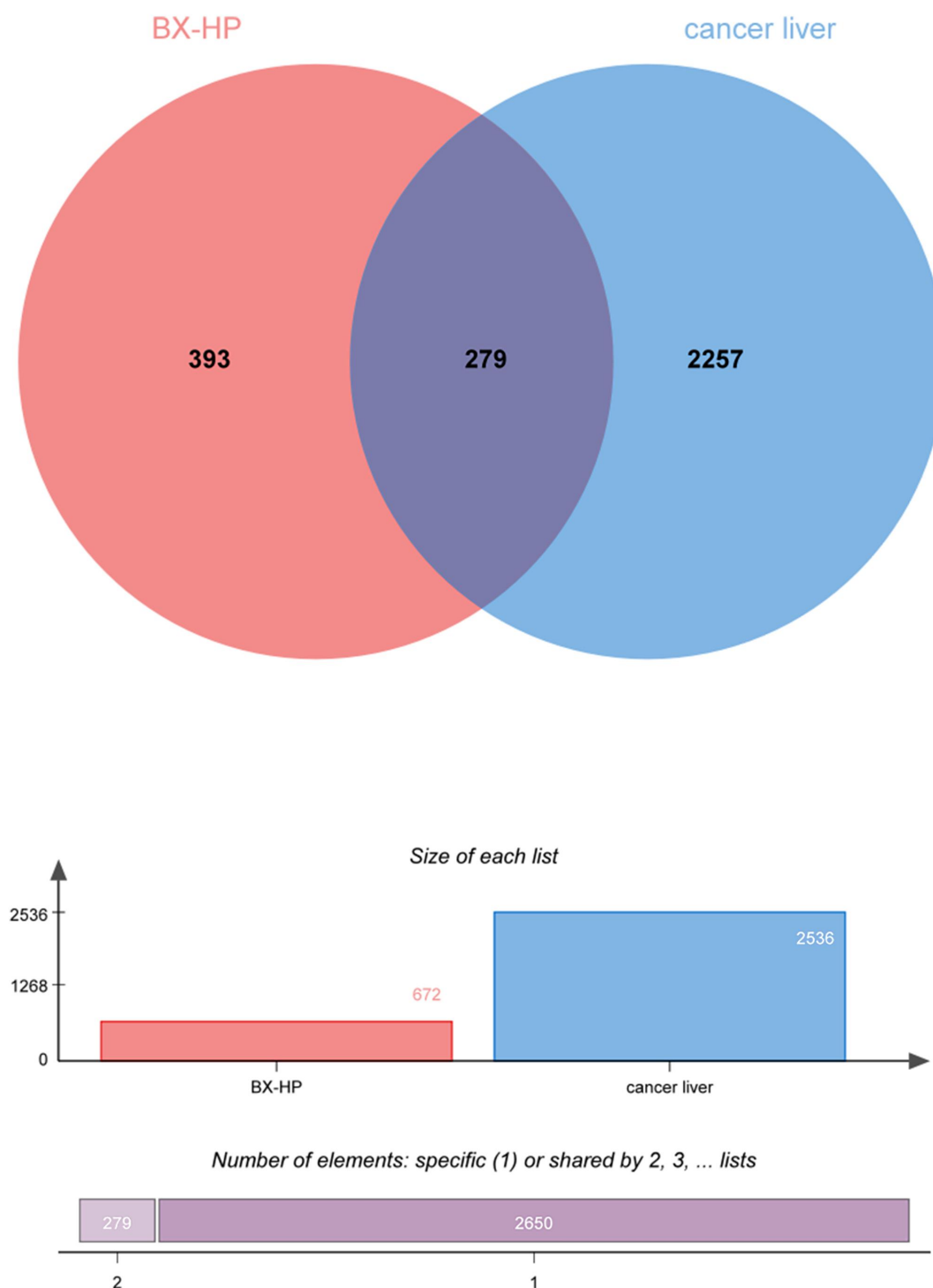
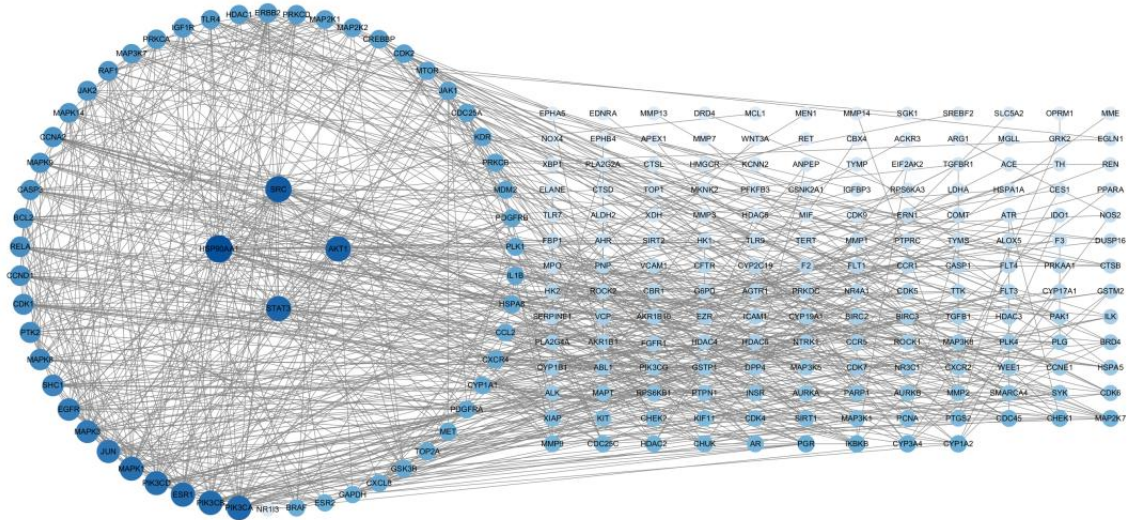


Figure 2 Herb pair *Pinellia ternata-Magnolia officinalis* targets overlap with hepatocellular carcinoma gene targets, Venn diagram

A



B

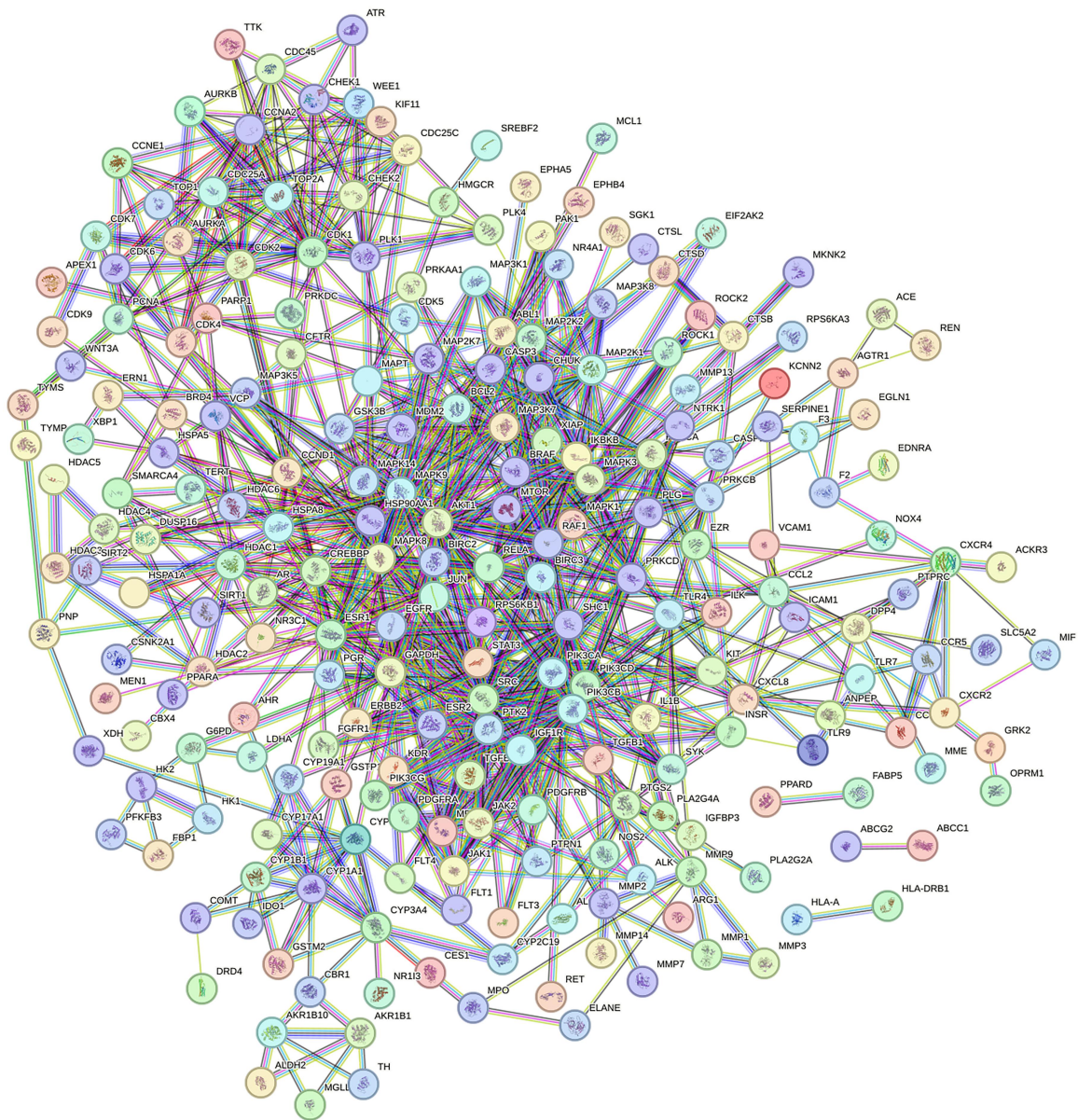


Figure 3 PPI protein network diagram. (A) Network diagram made with Cytoscape 3.10.1 (Darker colours represent higher values). (B) Network diagram made with STRING platform.

Construction and analysis of drug ingredient disease network

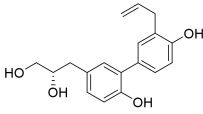
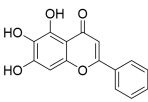
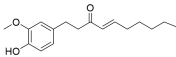
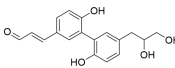
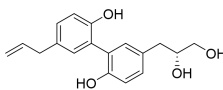
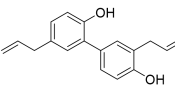
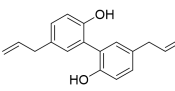
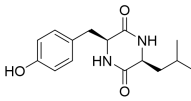
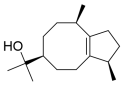
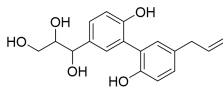
Import the intersection genes obtained from the Houpu and *Pinellia ternata* components with drugs and diseases into Cytoscape 3.10.1 to construct an "active ingredient disease target" network diagram (Figure 4), which included 323 nodes and 1142 edges. Using the CytoNCA plugin, components were filtered based on the "Degree," "Betweenness," and "Closeness" conditions. The components were visualized based on the Degree value, and the nodes increased as the Degree value increased. Select ten vital active ingredients (Table 2).

GO and KEGG enrichment analysis

A GO and KEGG enrichment analysis was performed using the David platform on 279 intersecting targets. GO is the abbreviation for gene ontology, used to annotate genes related to biological functions, pathways, and other products. Among them were 971 BP entries, mainly concentrated in protein physiology, negative regulation of the

apoptotic process, and protein auto-physiology. There were 118 CC entries, including cytosol, cycle flash, and nucleus, and 208 MF entries, mainly focused on protein serine/threonine/tyrosine kinase activity, protein kinase activity, and ATP binding. Calculate the count value and take the top 10 for a graphical analysis (Figure 5). A KEGG pathway enrichment analysis was performed on the 279 critical targets mentioned above using the DAVID database, resulting in 184 signal pathways. The top 20 signal pathways, including pathways in cancers, the MAPK signaling pathway, and the PI3K-AKT signaling pathway, were selected from high to low based on *P*-values and displayed as bubble charts. The size of the bubbles represents the number of enriched genes through the pathways, and the larger the bubbles are, the greater the number of enriched genes is. The colors of the bubbles represent the $-\log P$ value, which varies from red to green in size (Figure 6).

Table 2 Active constituents of herb pair *Pinellia ternata*-*Magnolia officinalis*

Compound	NO.	PubChem CID	Molecules name	Formula	Structure
1	HP10	5319203	magnolignan C	C ₁₈ H ₂₀ O ₄	
2	BX8	5281605	Baicalein	C ₁₅ H ₁₀ O ₅	
3	BX13	5281794	6-Shogaol	C ₁₇ H ₂₄ O ₃	
4	HP22	5319188	(E)-3-[3-[5-(2,3-dihydroxypropyl)-2-hydroxyphenyl]-4-hydroxyphenyl]prop-2-enal	C ₁₈ H ₁₈ O ₅	
5	HP15	5319201	Magnolignan A	C ₁₈ H ₂₀ O ₄	
6	HP5	72303	Honokiol	C ₁₈ H ₁₈ O ₂	
7	HP1	72300	Magnolol	C ₁₈ H ₁₈ O ₂	
8	BX25	15550385	cyclo-(leu-tyr)	C ₁₅ H ₂₀ N ₂ O ₃	
9	HP19	72607	[3R,(+)]-1,2,3,4,5,6,7,8-Octahydro- $\alpha,\alpha,3\beta,8\beta$ -tetramethyl-5 β -azulene methanol	C ₁₅ H ₂₆ O	
10	HP21	5319202	Magnolignan B	C ₁₈ H ₂₀ O ₅	

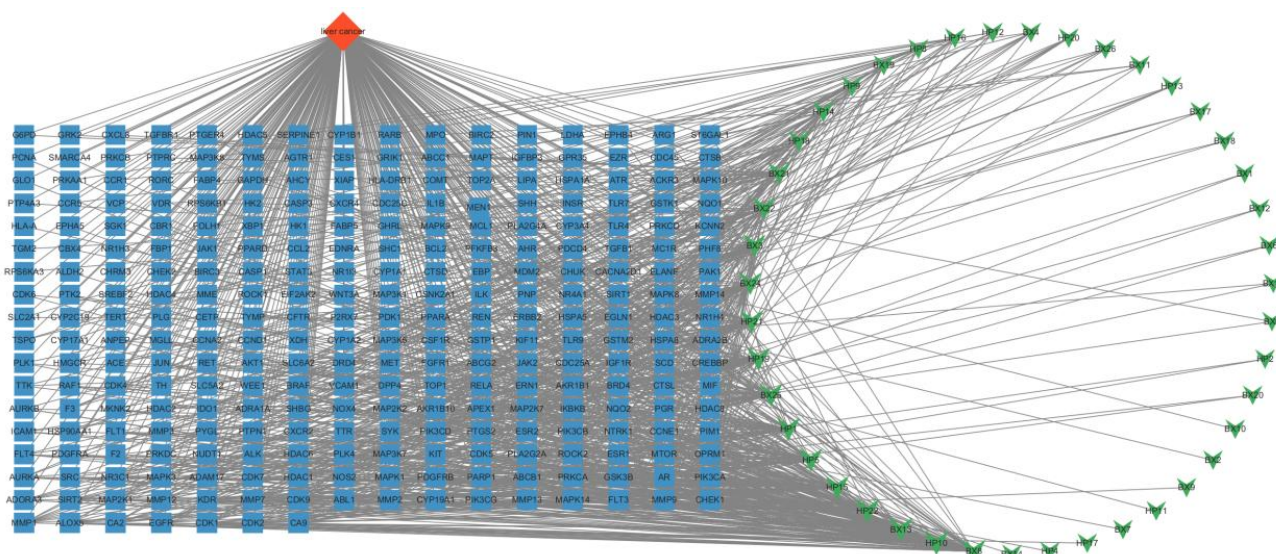


Figure 4 The network diagram of the active components-targets of BX-HP

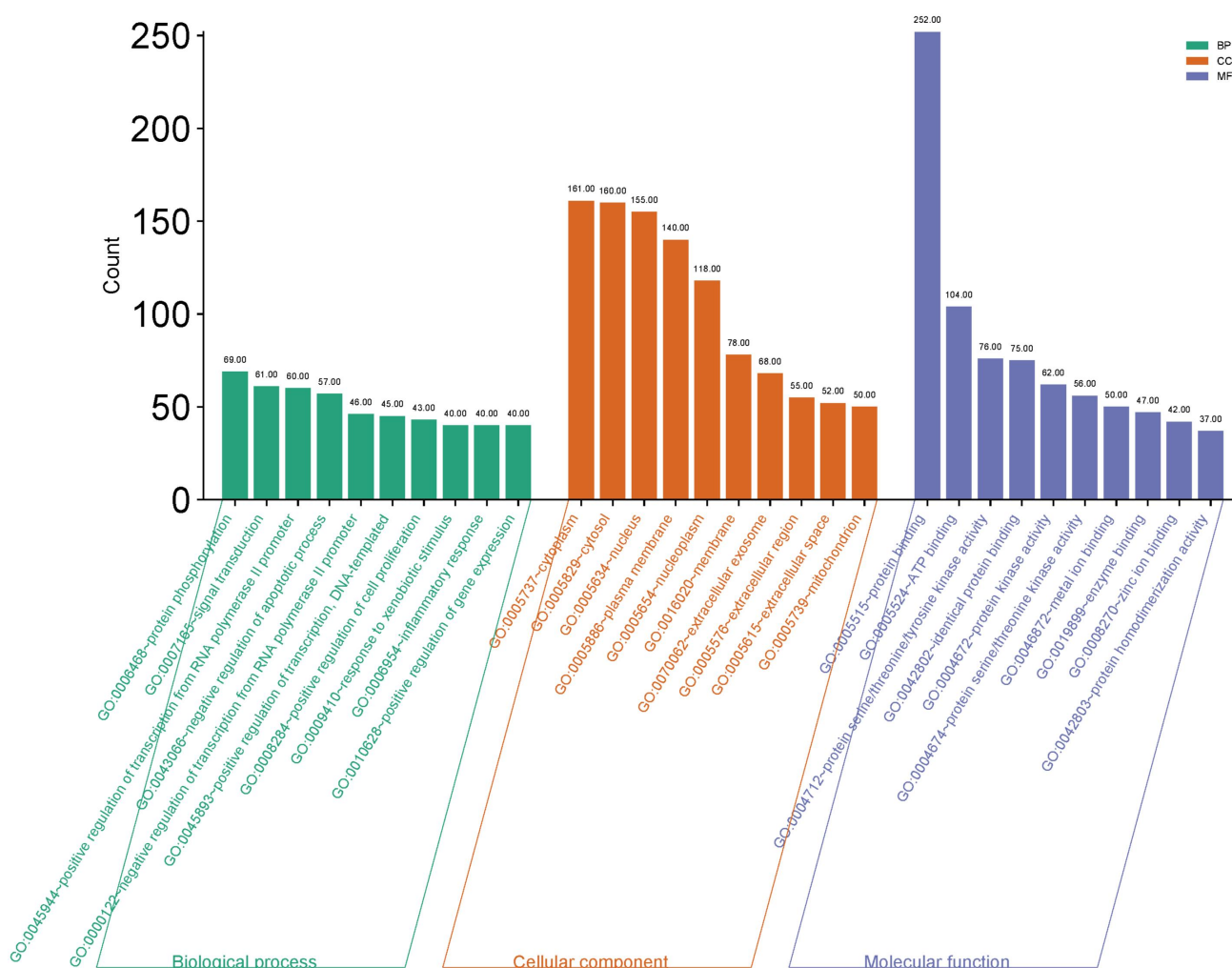


Figure 5 The analysis results of GO-BP-CC-MF

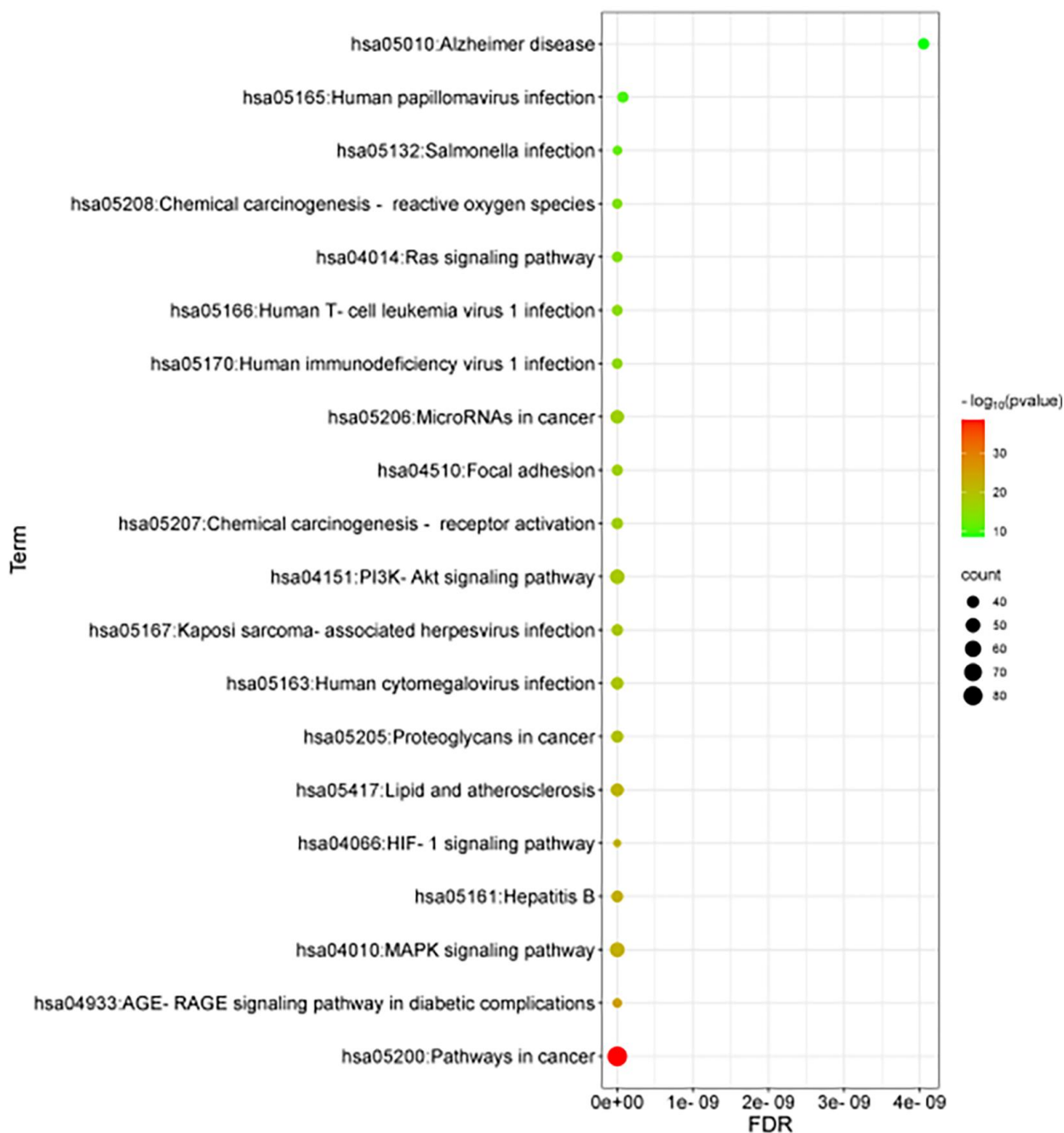


Figure 6 Bubbles in the enrichment analysis of the KEGG pathway

Molecular docking

Perform molecular docking on five core targets (HSP90AA1, SRC, AKT1, STAT3, and PIK3CA) and their corresponding compounds. It is generally believed that the lower the binding energy, the greater the possibility for the target proteins to bind to compounds and the more stable the binding conformation will be. By combining docking values, active ingredients and targets with better integration activity can be screened, with values < -4.25 kcal/mol indicating the binding activity between ligands and targets, values < -5.0 kcal/mol showing good binding activity, and values < -7.0 kcal/mol indicating more excellent docking activity [29].

The results showed that the five core targets (HSP90AA1, SRC, AKT1, STAT3, and PIK3CA) exhibited a good binding affinity with the

active ingredients, with all binding energies less than -4.25 kcal/mol. Specifically, the active ingredient that best binds to the core target HSP90AA1 is compound 2 (baicalein, BX8), with a binding energy of -7.8 kcal/mol. The active ingredient that best binds to the core target SRC is baicalein, with a binding energy of -8.6 kcal/mol. The active ingredient that best binds to the core target AKT1 is baicalein, with a binding energy of -9.5 kcal/mol. The active ingredient that best binds to the core target STAT3 is compound 2 (baicalein, BX8), with a binding energy of -6.4 kcal/mol. The active ingredient that best binds to the core target PIK3CA is baicalein, with a binding energy of -8.6 kcal/mol. All the five core targets (HSP90AA1, SRC, AKT1, STAT3, and PIK3CA) best bind to baicalein. Therefore, baicalein may be essential in treating liver cancer with the

herb pair *Pinellia ternata-Magnolia officinalis*. The results of docking between active ingredients and core target molecules are shown in

Figure 7. The visualization of partial molecular docking results is shown in Figure 8.

BC Target	Binding energy(kcal/mol)				
	HSP90AA1	SRC	AKT1	STAT3	PIK3CA
1	-6.8	-7.5	-8.8	-6.1	-7.7
2	-7.8	-8.6	-9.5	-6.4	-8.6
3	-5.6	-6.4	-7.8	-4.8	-6.7
4	-7.0	-7.3	-8.6	-6.3	-7.9
5	-6.7	-7.4	-8.2	-5.8	-6.9
6	-6.5	-7.5	-8.6	-5.8	-7.9
7	-6.4	-7.2	-8.2	-5.6	-7.4
8	-6.3	-6.9	-8.4	-5.7	-7.8
9	-6.9	-7.3	-8.5	-5.6	-7.9
10	-6.7	-7.5	-8.7	-6.1	-8.0

Figure 7 Heatmap for the docking results of the compounds with the proteins

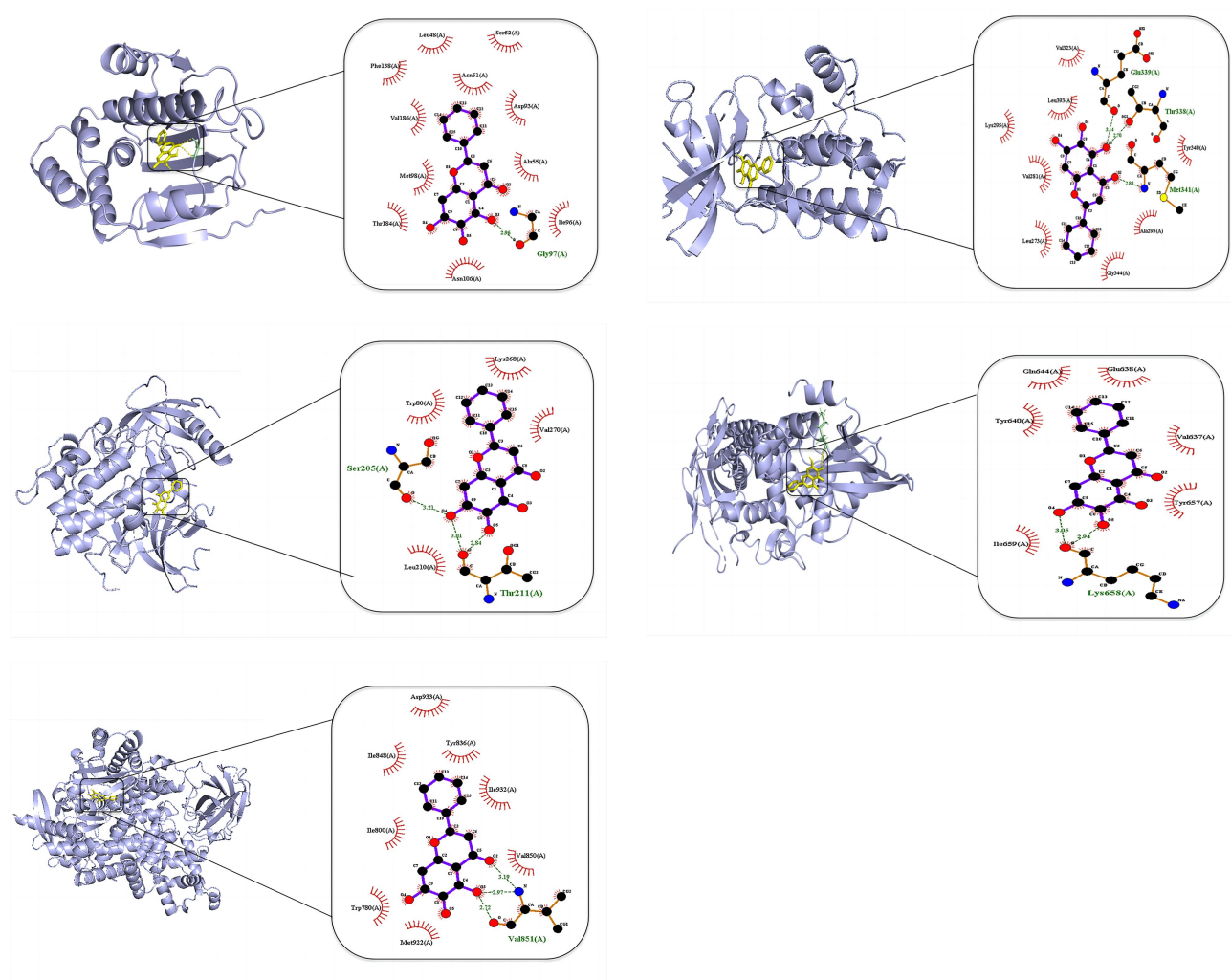


Figure 8 Visualization of component-target docking

In addition, amino acid interactions of all docking ligand-proteins were shown in Table 3–7. Baicalein has the lowest binding energy with the core target AKT1 through the most stable binding conformation-hydrogen bonding interactions: Ser205 (A), Thr211 (A), and hydrophobic interactions: Lys268 (A), Trp80 (A), Leu210 (A), Val270 (A), Lys268 (A).

We also assessed ligand-protein interactions using MD simulation analysis. A smaller RMSD value implies the stability of the ligand binding. We found that the RMSD values of the baicalein-AKT1 were generally less than 0.35 Å within 50 ns of simulation, and they became stable at approximately 15 ns, suggesting a sound binding of each complex (Figure 9).

Table 3 Amino acid interactions of active ingredient HSP90AA1

Compound	NO.	Hydrogen bonding	Hydrophobic interaction
1	HP10	Trp80(A); Leu213(A); Thr211(A)	Thr82(A); Tyr272(A); Val271(A); VAL270(A); Ser205(A); Ala212(A); Leu210(A); Leu264(A); Asp292(A); Gln79(A)
2	BX8	Ser205(A); Thr211(A)	Lys268(A); Trp80(A); Leu210(A); Val270(A)
3	BX13	Thr211(A); Trp80(A); Ile290(A)	Leu264(A); Tyr272(A); Lys268(A); Val270(A); Ser205(A); Leu210(A)
4	HP22	Val271(A); Phe293(A); Asp292(A); Trp80(A)	Thr211(A); Val270(A); Leu264(A); Thr82(A); Asn279(A); Thr291(A); Asp274(A); Gly294(A); Tyr272(A);
5	HP15	Val271(A); Ile290(A); Thr211(A)	Asp274(A); Thr82(A); Gln79(A); Leu264(A); Thr291(A); Leu210(A); Asp292(A); Tyr272(A); Arg273(A)
6	HP5	Tyr272(A)	Lys268(A); Val201(A); Ser205(A); Val271(A); Thr82(A); Gln79(A); Val270(A); Leu264(A); Trp80(A)
7	HP1	Val271(A)	Tlu82(A); Va270(A); Leu264(A); Gly294(A); Trp80(A); Asp292(A); Leu210(A); Tyr272(A); Asp274(A); Thr291(A); Phe293(A); Asn279(A)
8	BX25	Ile290(A); Thr211(A);	Gln79(A); Thr291(A); Tyr272(A); Leu210(A); Asp292(A); Trp80(A); Leu264(A); Thr82(A); Val270(A)
9	HP19	Trp80(A)	Val270(A); Lys268(A); Asp292(A); Leu210(A); Tyr272(A); Leu264(A); Val271(A)
10	HP21	Ser205(A); Thr211(A); Trp80(A)	Ala212(A); Leu213(A); Leu210(A); Lys268(A); Leu264(A); Tyr272(A);

Table 4 Amino acid interactions of active ingredient SRC

Compound	NO.	Hydrogen bonding	Hydrophobic interaction
1	HP10	Asp404(A); Met341(A)	Asn391(A); Lys295(A); Gly276(A); Leu393(A); Val281(A); Leu273(A); Tyr340(A); Ala403(A); Thr338(A); Ala390(A); Ala293(A)
2	BX8	Glu339(A); Thr338(A); Met341(A)	Val323(A); Leu393(A); Lys295(A); Val281(A); Leu273(A); Gly344(A); Ala293(A); Tyr340(A);
3	BX13	Thr338(A); Asn391(A); Ala390(A)	Leu273(A); Ala293(A); Val281(A); Val323(A); Lys295(A); Asp404(A); Leu393(A); Leu273(A)
4	HP22	Asp404(A)	Gly276(A); Lys295(A); Asn391(A); Ala403(A); Gly344(A); Leu393(A); Tyr340(A); Ala293(A); Thr338(A); Val281(A); Gly279(A)
5	HP15	Gly276(A); Asp404(A)	Glu280(A); Val281(A); Ala390(A); Ala293(A); Met341(A); Thr338(A); Ala403(A); Asn391(A); Leu393(A); Lys295(A); Gly279(A)
6	HP5	Asn391(A); Asp404(A)	Ala90(A); Gly276(A); Lys295(A); Ala293(A); Val281(A); Thr338(A); Met341(A); Leu393(A); Ala403(A)
7	HP1	Asp404(A)	Leu393(A); Met341(A); Ala293(A); Val281(A); Gly279(A); Gly276(A); Lys295(A); Asn391(A); Ala390(A); Ala403(A); Thr338(A)
8	BX25	Met341(A)	Tyr340(A); Ala293vLeu393(A); Val281(A); Gly274(A); Gln275(A); Lys295(A); Asp404(A); Gly276(A)
9	HP19	Thr338(A)	Gly274(A); Val281(A); Ala293(A); Val323(A); Lys295(A); Leu393(A); Met341(A); Gly344(A); Leu273
10	HP21	Arg858(A); Ile759(A)	Met766(A); Ala763(A); Glu762(A); Glu758(A); Leu788(A); Leu777(A); Asp855(A)

Table 5 Amino acid interactions of active ingredient AKT1

Compound	NO.	Hydrogen bonding	Hydrophobic interaction
1	HP10	Trp80(A); Leu213(A); Thr211(A)	Thr82(A); Tyr272(A); Val271(A); VAL270(A); Ser205(A); Ala212(A); Leu210(A); Leu264(A); Asp292(A); Gln79(A)
2	BX8	Ser205(A); Thr211(A)	Lys268(A); Trp80(A); Leu210(A); Val270(A)
3	BX13	Thr211(A); Trp80(A); Ile290(A)	Leu264(A); Tyr272(A); Lys268(A); Val270(A); Ser205(A); Leu210(A)
4	HP22	Val271(A); Phe293(A); Asp292(A); Trp80(A)	Thr211(A); Val270(A); Leu264(A); Thr82(A); Asn279(A); Thr291(A); Asp274(A); Gly294(A); Tyr272(A);
5	HP15	Val271(A); Ile290(A); Thr211(A)	Asp274(A); Thr82(A); Gln79(A); Leu264(A); Thr291(A); Leu210(A); Asp292(A); Tyr272(A); Arg273(A)
6	HP5	Tyr272(A)	Lys268(A); Val201(A); Ser205(A); Val271(A); Thr82(A); Gln79(A); Val270(A); Leu264(A); Trp80(A)
7	HP1	Val271(A)	Tlu82(A); Va270(A); Leu264(A); Gly294(A); Trp80(A); Asp292(A); Leu210(A); Tyr272(A); Asp274(A); Thr291(A); Phe293(A); Asn279(A)
8	BX25	Ile290(A); Thr211(A);	Gln79(A); Thr291(A); Tyr272(A); Leu210(A); Asp292(A); Trp80(A); Leu264(A); Thr82(A); Val270(A)
9	HP19	Trp80(A)	Val270(A); Lys268(A); Asp292(A); Leu210(A); Tyr272(A); Leu264(A); Val271(A)
10	HP21	Ser205(A); Thr211(A); Trp80(A)	Ala212(A); Leu213(A); Leu210(A); Lys268(A); Leu264(A); Tyr272(A);

Table 6 Amino acid interactions of active ingredient STAT3

Compound	NO.	Hydrogen bonding	Hydrophobic interaction
1	HP10	Met586(A); Leu608(A); Gly583(A)	Leu607(A); Tyr674(A); Ile677(A); Tyr584(A); Glu582(A); Leu673(A); Glu681(A); Ile585(A)
2	BX8	Lys658(A)	Gln644(A); Tyr640(A); Ile659(A); Tyr657(A); Val637(A); Glu638(A)
3	BX13	Leu577(A); Leu645(A)	Tyr686(A); Ala578(A); Asn646(A); Ser649(A); Met648(A); Tyr575(A); Ile576(A); Leu579(A)
4	HP22	Leu608(A); Tyr584(A); Glu582(A); Gly583(A); Met586(A)	Leu673(A); Tyr674(A); Glu681(A); Ile677(A); Ile585(A); Leu607(A)
5	HP15	Met586(A); Leu608(A); Gly583(A); Tyr584(A);	Ile585(A); Ile677(A); Tyr674(A); Leu607(A)
6	HP5	Tyr575(A)	Asn581(A); Ala578(A); Ser649(A); Tyr686(A); Ala651(A); Leu579(A); Ile576(A); Leu577(A)
7	HP1		Pro603(A); Ser668(A); Gly604(A); Met660(A); Glu625(A); Ile659(A); Asp661(A); Val667(A); Pro669(A); Val671(A)
8	BX25	Glu625(A); Ala662(A)	Gly604(A); Ser668(A); Pro669(A); Val667(A); Asp661(A); Trp623(A); Pro603(A)
9	HP19	Gly583(A)	Met586(A); Tyr584(A); Leu673(A); Ile585(A); Tyr674(A); Ser521(A); Gln524(A)
10	HP21	Glu638(A); Pro639(A)	Tyr640(A); Gln644(A); Thr641(A)

Table 7 Amino acid interactions of active ingredient PIK3CA

Compound	NO.	Hydrogen bonding	Hydrophobic interaction
1	HP10	Cys838(A); His670(A); Asn170(A)	Gly837(A); Phe666(A); Ser629(A); Arg662(A); Leu814(A); Pro835(A); Gln815(A); Arg818(A)
2	BX8	Val851(A)	Asp933(A); Ile848(A); Ile800(A); Trp780(A); Met922(A); Val850(A); Ile932(A); Tyr836(A)
3	BX13	Met811(A)	Tyr836(A); Pro835(A); Arg818(A); Gln815(A); Gln630(A); Ser629(A); Phe666(A); Ile633(A); Leu814(A)
4	HP22	Met811(A); Cys838(A)	His670(A); Phe666(A); Ser629(A); Asn756(A); Asn170(A); Arg662(A); Gln630(A); Gly837(A); Leu814(A); Gln815(A)
5	HP15	Arg693(A); Gly696(A); Glu109(A)	Leu113(A); Glu116(A); Thr303(A); Glu110(A); Pro305(A); Ala694(A)
6	HP5	Cys838(A); His670(A)	Pro835(A); Leu814(A); Arg818(A); Phe666(A); Arg662(A); Ser629(A); Gly837(A); Gln815(A)
7	HP1	His670(A); Gln630(A)	Ser629(A); Phe666(A); Arg662(A); Cys838(A); Leu839(A); Gln815(A); Leu632(A); Ile633(A)
8	BX25	His670(A); Tyr836(A)	Phe666(A); Ser629(A); Arg818(A); Pro835(A); Leu814(A); Gln815(A); Met811(A); Ile633(A)
9	HP19	Cys838(A)	Gly837(A); Gln815(A); Ile633(A); Ser629(A); Leu632(A); His670(A); Phe666(A); Leu839(A); Leu755(A)
10	HP21	His670(A); Met811(A); Arg818(A)	Ile633(A); Cys838(A); Leu839(A); Gln815(A); Pro835(A); Leu814(A); Tyr836(A); Phe666(A); Ser629(A)

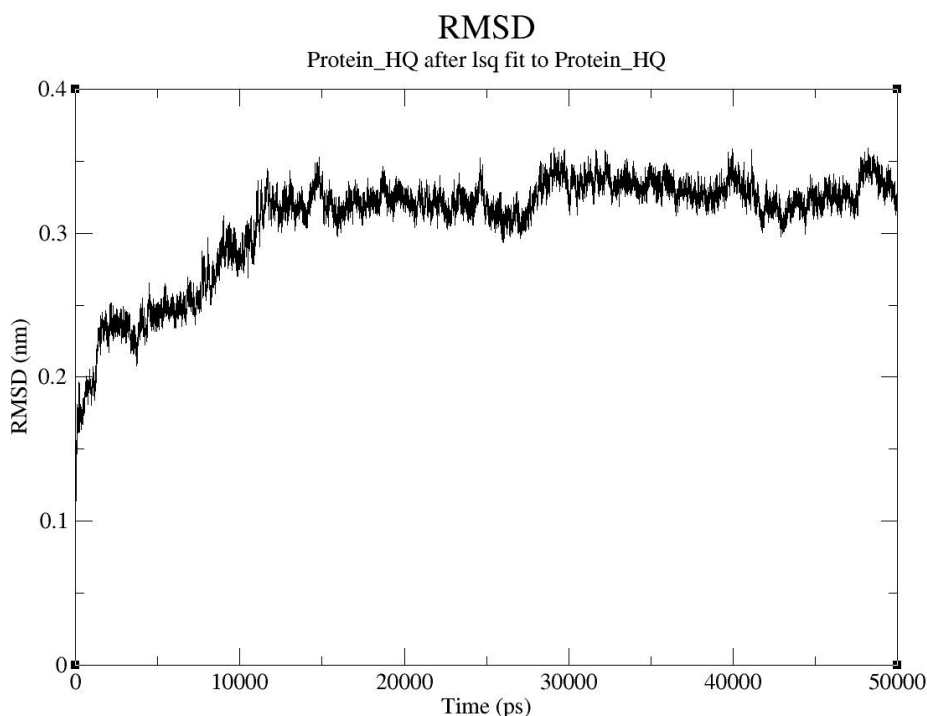


Figure 9 The RMSD values of the compound 2-AKT1

Discussion

In recent years, more and more research has been focused on discovering and developing drugs based on traditional Chinese medicine to study the action mechanism in treating liver cancer. In addition, network pharmacology and molecular docking simulation have played a significant role in predicting the therapeutic mechanism in this process. The anti-tumor mechanism of the herb pair *Pinellia ternata-Magnolia officinalis* in liver cancer was explored through network pharmacology. Finally, molecular docking simulations evaluated potential intermolecular interactions between core therapeutic targets and their corresponding compounds based on network results.

The chemical composition of *Pinellia ternata* is relatively complex, mainly containing effective components such as volatile oils, flavonoids, alkaloids, nucleosides, organic acids, etc. Animal and cell model experiments have shown that the anti-tumor effect of *Pinellia ternata* extract/effective fraction is definite. It has been proven that *Pinellia ternata* extract/effective fraction has significant inhibitory effects on various tumor cells such as liver cancer, cervical cancer, and gastric cancer. Research has found that *Magnolia officinalis* contains active ingredients such as lignans, alkaloids, and volatile oils, which have a good inhibitory effect on tumor cells such as lung cancer, liver cancer, and colon cancer. The network topology analysis results indicated ten active compounds, including magnolol C, baicalein, and 6-gingerol, might play a critical anti-cancer role. Baicalein is a common component of *Pueraria officinalis* and *Pinellia ternata*.

Research results suggest that baicalein is a potential candidate for treating hepatocellular carcinoma in cell viability assays, which show significant cytotoxicity on hepatocellular carcinoma cell lines H22, Bel-7404, and HepG2. Baicalein extract significantly inhibits the growth of H22 xenograft tumors without significant adverse effects on the body weight or liver and spleen weight index of ICR mice. The inhibition of tumor growth in mice treated with AKT β -shows a decreased expression of catenin, which is related to cyclin D1 in vitro [30]. 6-gingerol can induce the apoptosis of liver cancer cells, which has been demonstrated to mediate Wnt/inhibit the progression of liver cancer. β -Catenin signaling is a potential co-promoting drug for treating liver cancer [31]. These research findings and our findings suggest that the active ingredients of the herb pair *Pinellia*

ternata-Magnolia officinalis may be effective for treating liver cancer.

The PPI network shows that HSP90AA1, SRC, AKT1, STAT3, and PIK3CA are the core targets of the therapeutic effect of the herb pair *Pinellia ternata-Magnolia officinalis* on liver cancer. Our molecular docking results show that the core targets bind well with the key active ingredients of the *Pinellia ternata Magnolia officinalis* drug pair, with AKT1 showing the best docking binding energy. Therefore, the combination of *Pinellia ternata* with *Magnolia officinalis* may be used to treat liver cancer through the interactions between active ingredients and related proteins. Transcription activating factor 3 (STAT3) is a potential protein that can be activated in response to various cytokines and growth factors. HCC is one of the most common malignant tumors, and it has been reported that STAT3 can promote the proliferation, metastasis, survival, and angiogenesis of HCC cells [32]. The serine/threonine protein kinases of the RAC serine/threonine protein kinase (AKT) family, especially the AKT1 subtype, have been abnormally expressed in HCC cells and are highly correlated with cellular behavior, including proliferation, survival, metabolism, and tumorigenesis [33]. Studies have shown that the survival and proliferation of liver cancer cells are promoted through the differential regulation of AKT1 by mediating Notch1 expression. AKT1 is an oncogenic gene abnormally expressed in liver cancer cells and can be activated by PI3K, which plays a vital role in cell proliferation, survival, metabolism, and tumorigenesis. The overexpression of MiR-637 in liver cancer cells and its low expression in liver cancer tissues can reduce AKT1 expression and inhibit liver cancer cell proliferation and invasiveness by degrading AKT1. By inhibiting MiR-637 expression, liver cancer cell proliferation and invasiveness can be promoted by promoting AKT1 expression. In addition, the overexpression of AKT1 in hepatocellular carcinoma cells can partially reverse the inhibition of MiR-637 on liver cancer cell proliferation and invasiveness [34]. The activation of AKT1 can inhibit the expression of phosphatase and PTEN while inhibiting the activity of Notch1, and the inhibition of AKT1 can effectively promote the expression of Notch1, thereby inhibiting the proliferation of liver cancer cells, inducing cell apoptosis and cell cycle arrest [35]. Therefore, discovering AKT1 targets can provide a basis for learning new strategies for treating liver cancer. A Kaplan Meier survival analysis indicates that HSP90AA1 is a promising candidate gene that can serve as a diagnostic and prognostic biomarker for liver cancer

[36]. Our molecular docking results show that the core target matches well with the main components of the *Pinellia ternata* *Magnolia officinalis* drug pair, with AKT1 showing the best binding energy. Therefore, the herb pair *Pinellia ternata*-*Magnolia officinalis* could treat liver cancer by the interaction of active ingredients and liver cancer-related proteins.

A KEGG enrichment analysis showed a significant correlation between crucial drug targets and the regulation of pathways in cancers, the MAPK signaling pathway, and the PI3K-Akt signaling pathway. The mitogen-activated protein kinase/extracellular-signal-regulated kinase (MAPK/ERK) signaling pathway is often activated in cancers. In addition to gene mutations that cause sustained activation of effector molecules in the MAPK/ERK signaling pathway, other methods exist for starting the above pathway in cancers [37]. The PI3K-Akt signaling pathway is one of the classic signaling pathways related to the occurrence and development of liver cancer, whose activation can promote cancer cell proliferation, survival, migration and invasion, angiogenesis, and metabolism. MiR-30b-3p, which is significantly downregulated and positively correlated with the overall survival of hepatocellular carcinoma tissues and cells, can directly bind to the 3' untranslated region 3'-UTR of TRIM27 and downregulate TRIM27 expression, thereby inhibiting the activation of the PI3K/AKT signaling pathway while inhibiting the proliferation, migration, and invasion of liver cancer cells. Therefore, miR-30-3p may become a new biomarker for diagnosing and treating future hepatocellular carcinoma [38]. In hepatocellular carcinoma, NAD (P) H quinone dehydrogenase 1 (Nqo1) is highly overexpressed, and Nqo1 knockout can activate protein phosphatase 2A (PP2A) while inhibiting the activation of the PI3K/AKT and MAPK/ERK pathway, thereby inhibiting the expression of genes involved in glycolysis and glutathione degradation, blocking the metabolic adaptation of liver cancer cells, and thus inhibiting the proliferation of liver cancer cells as well as tumor growth. In addition, Nqo knockout also promotes PTEN expression through the ERK/CREB/c-Jun pathway, thereby inhibiting the activation of the PI3K/AKT signaling pathway. Therefore, Nqo1 may serve as a new therapeutic target to inhibit the proliferation of liver cancer cells, thereby exerting rich anti-liver therapeutic effects [39]. The PI3K/AKT signaling pathway may mediate the component target interaction in the therapeutic effect of herb pair *Pinellia ternata*-*Magnolia officinalis* on liver cancer.

Through molecular docking simulation, it was found that the core therapeutic targets exhibited a good docking affinity with active compounds of herb pair *Pinellia ternata*-*Magnolia officinalis*, with a binding energy of less than -4.25 kcal/mol. It is worth noting that baicalein has a high binding activity with core therapeutic targets such as HSP90AA1, SRC, AKT1, STAT3, and PIK3CA. Through molecular dynamics simulation to validate the results, we found that the RMSD value of baicalein-AKT1 is usually less than 0.35 Å within the simulated 50 ns, and they become stable at approximately 15 ns, indicating that the binding of each complex is sound. Therefore, we speculate that baicalein may be essential in treating liver cancer with the combination of the herb pair *Pinellia ternata*-*Magnolia officinalis*.

It is found in this article that the combination of the herb pair *Pinellia ternata*-*Magnolia officinalis* has the characteristics including multiple components and targets in the treatment mechanism of liver cancer, mainly involving ten vital active compounds, five core therapeutic targets, and three signaling pathways. The above research has preliminarily revealed the active ingredients and potential action mechanisms of the herb pair *Pinellia ternata*-*Magnolia officinalis* in treating liver cancer, providing inspiring information and a basis for further exploration.

References

1. Siegel RL, Miller KD, Wagle NS, et al. Cancer statistics, 2023. *CA A Cancer J Clinicians*. 2023;73(1):17–48. Available at: <http://doi.org/10.3322/caac.21763>
2. Zhang G. Breakthrough points and difficulties in traditional Chinese medicine treatment of primary liver cancer. *J Clin*

3. *Hepat*. 2021;37(9):2016–2024. Available at: <http://doi.org/10.3969/j.issn.1001-5256.2021.09.004>
4. Zhang DD. The Research on Drugs' Qi-Flavor Concerted Application in Treating Spleen-Stomach System Diseases of JinKuiYaoLve. *Fujian Univ Tradit Chin Med*. 2014. Available at: <http://doi.org/10.7666/d.Y2553666>
5. Tu SS, Guo Y. Study on the Mechanism of Chinese Medicine in the Treatment of Primary Hepatic Carcinoma. *Acta Chin Med*. 2021;36(04):695–698. Available at: <http://doi.org/10.16368/j.issn.1674-8999.2021.04.146>
6. Mao M, Yuan HX. Shennong's Classic of Materia Medica and Banxia (Pinelliae Rhizoma) in Application of Classical Formulas. *J Shandong Univ Tradit Chin Med*. 2022;46(06):673–678. Available at: <http://doi.org/10.16294/j.cnki.1007-659x.2022.06.001>
7. Mao R, He Z. Pinellia ternata (Thunb.) Breit: A review of its germplasm resources, genetic diversity and active components. *J Ethnopharmacol*. 2020;263:113252. Available at: <http://doi.org/10.1016/j.jep.2020.113252>
8. Yuan H. New thoughts on antitumor functional material base and mechanism of Pinelliae Rhizoma-Magnoliae Officinalis Cortex couplet medicines. *Chin Tradit Herbal Drugs*. 2018;1924–1931. Available at: <http://doi.org/10.7501/j.issn.0253-2670.2018.08.029>
9. Liu ZH, Sun XB. Network pharmacology: new opportunity for the modernization of traditional Chinese medicine. *Acta Pharm Sin*. 2012;47(6):696–703. Available at: <http://doi.org/10.16438/j.0513-4870.2012.06.001>
10. Luo T, LU Y, YAN S, et al. Network Pharmacology in Research of Chinese Medicine Formula: Methodology, Application and Prospective. *Chin J Integr Med*. 2020;26(1):72–80. Available at: <http://doi.org/10.1007/s11655-019-3064-0>
11. Fang S, Dong L, Liu L, et al. HERB: a high-throughput experiment-and reference-guided database of traditional Chinese medicine. *Nucleic Acids Res*. 2020;49(D1):D1197–1206. Available at: <http://doi.org/10.1093/nar/gkaa1063>
12. Daina A, Michielin O, Zoete V. SwissTargetPrediction: updated data and new features for efficient prediction of protein targets of small molecules. *Nucleic Acids Res*. 2019;47(W1):W357–364. Available at: <http://doi.org/10.1093/nar/gkz382>
13. Daina A, Michielin O, Zoete V. SwissADME: a free web tool to evaluate pharmacokinetics, drug-likeness and medicinal chemistry friendliness of small molecules. *Sci Rep*. 2017;7(1):42717. Available at: <http://doi.org/10.1038/srep42717>
14. UniProt Consortium. UniProt: a worldwide hub of protein knowledge. *Nucleic Acids Res*. 2019;47(D1):D506–515. Available at: <http://doi.org/10.1093/nar/gky1049>
15. Fishilevich S, Zimmerman S, Kohn A, et al. Genic insights from integrated human proteomics in GeneCards. *Database*. 2016;2016:baw030. Available at: <http://doi.org/10.1093/database/baw030>
16. Wang Y, Zhang S, Li F, et al. Therapeutic target database 2020: enriched resource for facilitating research and early development of targeted therapeutics. *Nucleic Acids Res*. 2019;48(D1):D1031–D1041. Available at: <http://doi.org/10.1093/nar/gkz981>
17. Wishart DS, Feunang YD, Guo AC, et al. DrugBank 5.0: a major update to the DrugBank database for 2018. *Nucleic Acids Res*. 2018;46(D1):D1074–D1082. Available at: <http://doi.org/10.1093/nar/gkz981>
18. Piñero J, Ramírez-Angueta JM, Sañch-Pitarch J, et al. The DisGeNET knowledge platform for disease genomics: 2019 update. *Nucleic Acids Res*. 2019;48(D1):D845–855. Available at: <http://doi.org/10.1093/nar/gkz1021>
19. Szklarczyk D, Gable AL, Lyon D, et al. STRING v11:

- protein–protein association networks with increased coverage, supporting functional discovery in genome-wide experimental datasets. *Nucleic Acids Res.* 2018;47(D1):D607–613. Available at: <http://doi.org/10.1093/nar/gky1131>
19. Dennis G Jr, Sherman BT, Hosack DA, et al. DAVID: Database for Annotation, Visualization, and Integrated Discovery. *Genome Biol.* 2003;4(9):R60. Available at: <http://doi.org/10.1186/gb-2003-4-9-r60>
 20. Bardou P, Mariette J, Escudie F, et al. jvenn: an interactive Venn diagram viewer. *BMC Bioinformatics.* 2014;15(1):293. Available at: <http://doi.org/10.1186/1471-2105-15-293>
 21. Joosten RP, te Beek TAH, Krieger E, et al. A series of PDB related databases for everyday needs. *Nucleic Acids Res.* 2010;39(Database):D411–419. Available at: <http://doi.org/10.1093/nar/gkq1105>
 22. Kim S, Thiessen PA, Cheng T, et al. Literature information in PubChem: associations between PubChem records and scientific articles. *J Cheminform.* 2016;8(1):32. Available at: <http://doi.org/10.1186/s13321-016-0142-6>
 23. Ru J, Li P, Wang J, et al. TCMSP: a database of systems pharmacology for drug discovery from herbal medicines. *J Cheminform.* 2014;6(1):13. Available at: <http://doi.org/10.1186/1758-2946-6-13>
 24. Otasek D, Morris JH, Bouças J, et al.. Cytoscape Automation: empowering workflow-based network analysis. *Genome Biol.* 2019;20(1):185. Available at: <http://doi.org/10.1186/s13059-019-1758-4>
 25. Morris GM, Huey R, Lindstrom W, et al. AutoDock4 and AutoDockTools4: Automated docking with selective receptor flexibility. *J Comput Chem.* 2009;30(16):2785–2791. Available at: <http://doi.org/10.1002/jcc.21256>
 26. Yuan S, Chan HCS, Hu Z. Using PyMOL as a platform for computational drug design. *WIREs Comput Mol Sci.* 2017;7(2):e1298. Available at: <http://doi.org/10.1002/wcms.1298>
 27. Evans DA. History of the Harvard ChemDraw Project. *Angew Chem Int Ed.* 2014;53(42):11140–11145. Available at: <http://doi.org/10.1002/anie.201405820>
 28. Ma B, Ning J, Wang F, et al. Molecular Mechanism of the Therapeutic Effect of Peach Blossom against Constipation: An Exploratory Study Based on Network Pharmacology Analysis and Molecular Docking Verification. *Evid Based Complement Alternat Med.* 2023;2023:1–14. Available at: <http://doi.org/10.1155/2023/8577485>
 29. Hsin KY, Ghosh S, Kitano H. Combining machine learning systems and multiple docking simulation packages to improve docking prediction reliability for network pharmacology. *PLoS One.* 2013;8(12):e83922. Available at: <http://doi.org/10.1371/journal.pone.0083922>
 30. Zheng Y, Yin L, Grahn THM, et al. Anticancer Effects of Baicalein on Hepatocellular Carcinoma Cells. *Phytother Res.* 2014;28(9):1342–1348. Available at: <http://doi.org/10.1002/ptr.5135>
 31. Zhang Y, Wang J, Qu Y, et al. 6-Shogaol Suppresses the Progression of Liver Cancer via the Inactivation of Wnt/ β -Catenin Signaling by Regulating TLR4. *Am J Chin Med.* 2021;49(08):2033–2048. Available at: <http://doi.org/10.1142/S0192415X21500968>
 32. Tan ZB, Fan HJ, Wu YT, et al. Rheum palmatum extract exerts anti-hepatocellular carcinoma effects by inhibiting signal transducer and activator of transcription 3 signaling. *J Ethnopharmacol.* 2019;232:62–72. Available at: <http://doi.org/10.1016/j.jep.2018.12.019>
 33. Chen J, Liang J, Liu S, et al. Differential regulation of AKT1 contributes to survival and proliferation in hepatocellular carcinoma cells by mediating Notch1 expression. *Oncol Lett March.* 2018. Available at: <http://doi.org/10.3892/ol.2018.8193>
 34. DU SM. The SNHG16/miR-30a axis promotes breast cancer cell proliferation and invasion by regulating RRM2. *Neo.* 2020;67(03):567–575. Available at: http://doi.org/10.4149/neo_2020_190625N550
 35. Shi W, Feng L, Dong S, et al. FBXL6 governs c-MYC to promote hepatocellular carcinoma through ubiquitination and stabilization of HSP90AA1. *Cell Commun Signal.* 2020;18(1):100. Available at: <http://doi.org/10.1186/s12964-020-00604-y>
 36. Moon H, Park H, Chae MJ, et al. Activated TAZ induces liver cancer in collaboration with EGFR/HER2 signaling pathways. *BMC Cancer.* 2022;22(1):423. Available at: <http://doi.org/10.1186/s12885-022-09516-1>
 37. Moon H, Ro SW. MAPK/ERK Signaling Pathway in Hepatocellular Carcinoma. *Cancers.* 2021;13(12):3026. Available at: <http://doi.org/10.3390/cancers13123026>
 38. Dimri M, Humphries A, Laknaur A, et al. NAD(P)H Quinone Dehydrogenase 1 Ablation Inhibits Activation of the Phosphoinositide 3-Kinase/Akt Serine/Threonine Kinase and Mitogen-Activated Protein Kinase/Extracellular Signal-Regulated Kinase Pathways and Blocks Metabolic Adaptation in Hepatocellular Carcinoma. *Hepatology.* 2019;71(2):549–568. Available at: <http://doi.org/10.1002/hep.30818>
 39. Lou K, Chen N, Li Z, et al. MicroRNA-142-5p Overexpression Inhibits Cell Growth and Induces Apoptosis by Regulating FOXO in Hepatocellular Carcinoma Cells. *Oncol res.* 2017;25(1):65–73. Available at: <http://doi.org/10.3727/096504016X14719078133366>